Separation Science and Technology
Publication details, including instructions for authors and subscription information:
http://www.informaworld.com/smpp/title~content=t713708471

Insights into the Transport of Toluene and Phenol Through Organic Solvent Nanofiltration Membranes

S. J. Han[a]; S. S. Luthra[a]; L. Peeva[a]; X. J. Yang[a]; A. G. Livingston[a]
[a] Department of Chemical Engineering & Chemical Technology, Imperial College of Science, Technology and Medicine, London, United Kingdom

Online publication date: 15 April 2003

To cite this Article Han, S. J. , Luthra, S. S. , Peeva, L. , Yang, X. J. and Livingston, A. G.(2003) 'Insights into the Transport of Toluene and Phenol Through Organic Solvent Nanofiltration Membranes', Separation Science and Technology, 38: 9, 1899 — 1923
To link to this Article: DOI: 10.1081/SS-120020126
URL: http://dx.doi.org/10.1081/SS-120020126

MARCEL DEKKER, INC. • 270 MADISON AVENUE • NEW YORK, NY 10016

SEPARATION SCIENCE AND TECHNOLOGY
Vol. 38, No. 9, pp. 1899–1923, 2003

Insights into the Transport of Toluene and Phenol Through Organic Solvent Nanofiltration Membranes

S. J. Han, S. S. Luthra, L. Peeva, X. J. Yang, and A. G. Livingston*

Department of Chemical Engineering & Chemical Technology, Imperial College of Science, Technology and Medicine, London, United Kingdom

ABSTRACT

Overall mass transfer coefficients (OMTCs) during membrane solvent extraction (MSE) for a microfiltration membrane Accurel, an organic solvent nanofiltration (OSN) membrane MPF 50, and silicone rubber were investigated with a hydrophilic solute (phenol) and a hydrophobic solute (toluene) in a membrane solvent extractor. Decanol was used to extract phenol or toluene from water. In MSE of phenol from water, MPF 50 has an OMTC intermediate between Accurel and silicone rubber, and has a much higher breakthrough pressure than Accurel. For MPF 50, it was observed that the solute–membrane interaction makes a major

*Correspondence: A. G. Livingston, Department of Chemical Engineering & Chemical Technology, Imperial College of Science, Technology and Medicine, Prince Consort Road, London SW7 2BY, United Kingdom; Fax: 00-44-20-75945629; E-mail: a.livingston@ic.ac.uk.

DOI: 10.1081/SS-120020126 0149-6395 (Print); 1520-5754 (Online)

MARCEL DEKKER, INC. • 270 MADISON AVENUE • NEW YORK, NY 10016

contribution to the mass transport of hydrophobic compounds, such as toluene, through the membrane. This suggests that solution-diffusion type models may be more appropriate than pore-flow models for describing transport of solvents through these kinds of membranes.

Key Words: Nanofiltration; Extraction; Solution diffusion.

INTRODUCTION

In membrane solvent extraction (MSE), there are two main kinds of membranes used: porous and nonporous.[1] The separation principles are generally accepted as quite different for these two kinds of membranes. For porous membranes, MSE proceeds with a hydrophilic or hydrophobic membrane wetted by one phase and not wetted by the other phase. The two phases contact each other at the mouth or just inside the pores and mass transport of solutes between the phases takes place. In principle, the porous membrane in this process does not play any role in the selectivity of the process. It simply prevents the dispersion of one phase into another. In contrast, with nonporous membranes, the solute can pass only if it dissolves into the membrane material. The extent of such solubility is determined by the affinity between the membrane and the solute. The solute within the membrane is transported from one side to the other side by a driving force, such as a chemical potential difference across the membrane.

Among porous membranes, microfiltration membranes have widely been applied for MSE processes.[2–9] Microfiltration membranes have pore sizes in the range of 0.1 to 10 microns, and so offer relatively low mass transfer resistance. However, because microfiltration membranes have these large pore sizes, their breakthrough pressure (calculated theoretically by the Laplace–Young equation) is usually low (only a few bars). Low breakthrough pressure creates problems of operating stability during MSE with microfiltration membranes. Pressure drops resulting from the need to pass fluids along the membranes, and the effects of surface-active species lowering breakthrough pressure by reducing interfacial tensions, make it a tough task to prevent breakthrough from taking place in most real processes. This problem has been noted for Celgard microfiltration hollow fibers, and composite microfiltration membranes have been proposed to provide higher breakthrough pressures.[2,3]

Nonporous membranes were proposed for carrying out extraction by Lee et al,[10] which led to related later work.[11–16] Because there are no permanent pores in this kind of membrane, operating stability can be improved when the working pressure is less than the bursting pressure of the membrane. However,

there is a negative effect on the mass-transfer rate due to relatively low diffusion coefficients of solutes in nonporous membranes.[14]

Organic solvent nanofiltration (OSN) membranes have recently appeared.[17–23] Given their high breakthrough pressure and solvent resistance, it would be interesting to investigate how well OSN membranes behave in MSE. In this study, a comparison of the breakthrough pressure and the overall mass transfer coefficient (OMTC) was made among a range of microfiltration, OSN, and nonporous membranes. Phenol was chosen as a solute in this study because it has been widely used by previous researchers into MSE.[4,5,24] It provides a good benchmark. This study also hoped to further understand the transport mechanism through OSN membranes. In MSE with porous membranes, it is generally assumed that mass transport takes place along the membrane pores without any contribution of diffusion through the membrane material. We sought to find out whether the membrane material made any contribution to mass transport for OSN membranes. Toluene was selected as a second solute for comparison with phenol because it is classified as relatively hydrophobic, whereas phenol is relatively hydrophilic; the two have similar molecular weights. *n*-Decanol was used as the solvent to extract these solutes from aqueous solution.

THEORY

Resistances-in-Series Model

The resistances-in-series model is widely used to describe the transport of a penetrant through a membrane with liquid films on both sides.[2] The model was applied in this study. The permeation rate is characterised by the overall mass transfer coefficient based on concentration driving force, k_{ov}. To describe the mass transport in the membrane solvent extractor, the following main assumptions were made.

1. Equilibrium distributions of the solute exist across all phase interfaces.
2. There is no convective flow in the membrane pores and the diffusion describes the transport in the membrane pores.
3. There is no mass accumulation within the membrane.
4. The interfacial solute concentrations in solutions are the same for the membrane-solution and pore-solution interfaces.

Mass transport in MSE is shown as a diagram in Fig. 1a. Figures 1b and 1c demonstrate two possible configurations of mass transport in OSN membranes, that is, with or without discrete pores in the top, separating layer.

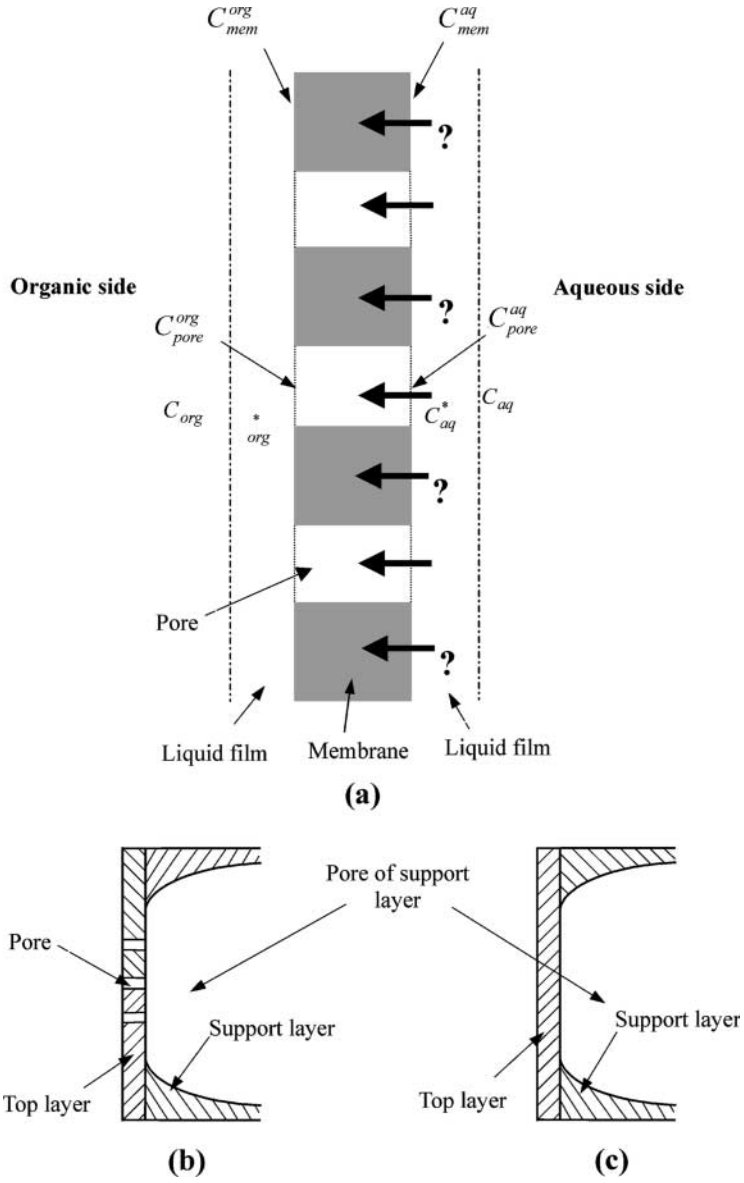

Figure 1. Mass transport through porous membranes (a); and two possible configurations of NF composite membranes with/without pores across the top layer within support layer pores, (b) and (c), respectively.

With these assumptions, the following equation describes the mass transfer rate of the solute.

$$\begin{aligned} F &= k_{aq}A\left(C_{aq} - C^{*}_{aq}\right) \text{ (aqueous side)} \\ &= \frac{D_{mem}A(1-\varepsilon)}{l}\left(C^{aq}_{mem} - C^{org}_{mem}\right) \\ &\quad + \frac{D_{pore}A\varepsilon}{l\tau}\left(C^{aq}_{pore} - C^{org}_{pore}\right) \text{ (membrane)} \\ &= k_{org}A\left(C^{*}_{org} - C_{org}\right) \text{ (organic side)} \end{aligned} \tag{1}$$

Rearranging Eq. (1) gives

$$F = k^{aq}_{ov}\,A\left(C_{aq} - \frac{C_{org}}{P^{org}_{aq}}\right) \tag{2}$$

Case A: For hydrophobic porous membranes, pores are filled with organic solvents, for example the decanol in this study. The overall mass-transfer coefficient k^{aq}_{ov} is expressed as

$$\frac{1}{k^{aq}_{ov}} = \frac{1}{k_{aq}} + \frac{l}{D_e\,P^{org}_{aq}} + \frac{1}{k_{org}\,P^{org}_{aq}} \tag{3}$$

With the definition of D_e as

$$D_e = (1-\varepsilon)D_{mem}\,P^{mem}_{org} + \frac{D_{pore}\varepsilon}{\tau} \tag{4}$$

where D_e is the effective diffusion coefficient in the membrane, the first term on the right side of Eq. (4) is the contribution of mass transport through the membrane material, and the second term is the contribution of mass transport in the pores. Note that if the scenario depicted in Fig. 1c exists, all transport is through the top, separating layer material; whereas if scenario in Fig. 1b exists, transport may be through both the pores and the top, separating layer material.

Case B: For hydrophilic porous membranes with water in the pores, the overall mass transfer coefficient k_{ov} is expressed as

$$\frac{1}{k^{aq}_{ov}} = \frac{1}{k_{aq}} + \frac{l}{D_e} + \frac{1}{k_{org}\,P^{org}_{aq}} \tag{5}$$

Defining D_e as

$$D_e = (1 - \varepsilon)D_{mem}P_{aq}^{mem} + \frac{D_{pore}\varepsilon}{\tau} \tag{6}$$

where D_e is the effective diffusion coefficient in the membrane, and the first and second terms can be explained as for Eq. (4).

Determination of the Overall Mass Transfer Coefficient (OMTCs)

In this study, aqueous solutions containing either phenol or toluene and pure decanol were recycled through respective half-cells with the membrane as a barrier, as shown in Fig. 2. The details of the experiments are described in the next section. For the calculation of OMTCs, it was assumed that both the aqueous solution and decanol solutions were well-mixed and that the recirculation rate through the halfcells was sufficiently high that there were no concentration gradients in the cells. Based on a mass balance for the solute we get:

$$C_{org} = \frac{V_{aq}}{V_{org}}\left(C_{aq,0} - C_{aq}\right) \tag{7}$$

and

$$-V_{aq}\frac{dC_{aq}}{dt} = k_{ov}^{aq}A\left(C_{aq} - \frac{C_{org}}{P_{aq}^{org}}\right) \tag{8}$$

Substituting Eq. (7) into Eq. (8) and integrating the expression, the following equation is derived

$$\frac{k_{ov}^{aq}A}{V_{aq}}t = \frac{1}{1+\beta}\ln\left(\frac{C_{aq,0}}{(1+\beta)C_{aq} - \beta C_{aq,0}}\right) \tag{9}$$

in which

$$\beta = \frac{V_{aq}}{P_{aq}^{org}V_{org}}$$

It can be seen that the plot of the term on the right side of Eq. (9) against time will yield a linear line with a slope of $\frac{k_{ov}^{aq}A}{V_{aq}}$. Therefore, the value of k_{ov}^{aq} can be obtained for the given values of A and V_{aq}.

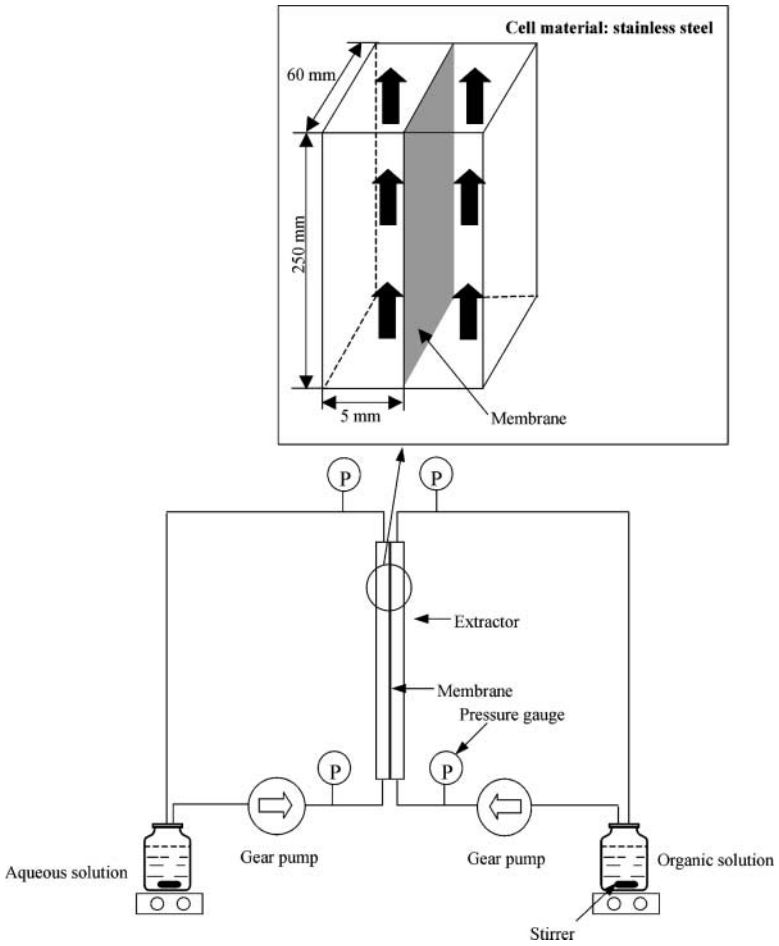

Figure 2. Diagram of the experimental set-up.

EXPERIMENTAL

Reagents

In this study, all chemicals (analytical grade) were supplied by Lancaster Synthesis Ltd, UK. Table 1 lists the physical properties of the compounds used in this study.

Table 1. Physical properties of chemicals at 20°C.

Compound	Density (kgm^{-3})	Solubility in water (gl^{-1})	Viscosity (Pa.s) $\times 10^3$	Diffusion coefficient in water[a] (m^2s^{-1}) $\times 10^{10}$	Diffusion coefficient in decanol[a] (m^2s^{-1}) $\times 10^{10}$
Phenol	—	87	—	8.9	1.22
Toluene	—	0.5	—	8.5	1.23
n-decanol	830	0.036	13.58	—	—

[a] According to the Wilke–Chang equation.[27]

Membranes

A range of microfiltration, OSN, and nonporous membranes were tested in this study. Table 2 lists the membranes and their properties. Accurel PP (polypropylene) 2E was supplied by Membrane GmbH, Germany and MPF 50 by Koch, US. Silicone rubber, composed of 30 wt% fumed silica and 70 wt% poly(dimethylsiloxane), or PDMS, was bought from Silex Ltd, UK. The thickness quoted for the OSN membranes is the total thickness of the top layer and support. The thickness of the active top layer can be estimated only from the electron micrographs.

Partition Coefficient and Distribution Coefficient

The procedure described by Brookes and Livingston[11] was followed to measure partition coefficients of phenol and toluene between the membranes

Table 2. Data sheet for membranes used in this study.

Membrane	Type	Separating layer	Support	Break through pressure (bar)	Pore size (μm)	Total thickness (mm)
Accurel	Microfiltration	Polypropylene	None	1.1*	0.2	0.15
MPF 50	Nanofiltration	Polydimethyl siloxane	Polyacrylo nitrile	30	Not available	0.25
Silicone rubber	Nonporous	Polydimethyl siloxane + silica	None	None	Nonporous	0.70

*Provided by the manufacturer.

and water. In the measurement of the partition coefficient of each membrane, three membrane samples were prepared in addition to a blank sample not containing membrane.

The distribution coefficient of toluene between decanol and water was measured by conventional solvent extraction. De-ionized water was mixed together with decanol containing toluene at a volume ratio of 1:1 and then allowed to phase separate. Toluene concentration in the aqueous solution after extraction was analyzed using a gas chromatograph (GC). The distribution coefficient was obtained from the ratio of toluene concentrations in the two phases.

Breakthrough Pressure

A similar experimental cell to the one described by Zha et al.[25] was used to measure the breakthrough pressure of MPF 50. The effective diameter of the membrane sample is 50 mm in the equipment utilized. Water was used to measure the breakthrough pressure of MPF 50.

Analytical Techniques

A GC with a flame ionization detector (Autosystem XL, Perkin Elmer, US) fitted with a 30-m long megabore column type DB 5 (J. W. Scientific, UK) was used to analyze toluene and phenol concentrations in aqueous solutions. Sample solutions were extracted into dichloromethane containing chlorobenzene as an internal standard. A 1μL sample of this extract was injected into the GC to analyze its concentration. The GC was run at a temperature program from 60° to 90°C at a rate of 10°C min^{-1}. The coefficient of variation of this assay (over 5 measurements) was 5% at 0.1 $g\,l^{-1}$.

Phenol and toluene concentrations in decanol were measured by a UV spectrophotometer (Shimadzu Corporation, Japan). The absorption wavelength selected for phenol and toluene detection was 270 nm. The coefficient of variation of this assay (over 5 measurements) was less than 5% at 0.3 $g\,l^{-1}$ for toluene and 4.7 $g\,l^{-1}$ for phenol.

Experimental Set-up

Figure 2 shows the diagram of the experimental set-up for measurements of OMTCs. The rig is made of two half-cells of stainless steel. A membrane

sheet with an effective area of $0.015\,m^2$ was installed between the two half-cells and sealed with two Viton 'O' rings.

Aqueous solutions containing either phenol or toluene, and an organic phase decanol, were recycled by two gear pumps on opposite sides of the membrane. The flow of the aqueous and organic phases was concurrent upward in this study. For all the experiments with phenol, the initial phenol concentration was $9.4\,g\,l^{-1}$ ($0.1\,mol\,l^{-1}$). The volumes of both aqueous phenol solution and decanol were 300 mL. Initial toluene concentrations in the feed solution were in the range of 250 to $400\,mg\,l^{-1}$. Because toluene is volatile, its initial concentrations in the extractor were determined by sampling the solutions as soon as the experiments started. The volumes of aqeuous toluene solution and decanol were 1000 mL and 500 mL, respectively. The flow rate was $10\,mL\,s^{-1}$ on the aqueous side and $1.5\,mL\,s^{-1}$ on the decanol side.

Before each experiment with porous membranes, the phase with affinity for the membrane (decanol) was recycled through one half-cell in the extractor to fill membrane pores with the wetting phase. Then, the non-wetting phase was recycled through the other half-cell with a higher pressure. That decanol was the preferred wetting phase for MPF 50 was verified by testing the membranes in the breakthrough pressure experimental cell.

RESULTS AND DISCUSSION

Breakthrough Pressure

The breakthrough pressure was measured for MPF 50 by using de-ionized water and the value is shown in Table 2. As shown in Table 2, the breakthrough pressure of MPF 50 is much higher than the microfiltration membrane Accurel. For a uniformly cylindrical pore, the breakthrough pressure is determined by the Laplace–Young equation.

$$P_b = \frac{2\gamma\cos\theta}{r} \tag{10}$$

where γ is the interfacial tension, θ the contact angle, and r the capillary radius. If it was assumed that except for r, two other parameters in Eq. (10) are constant, the ratio of breakthrough pressure in MPF 50 (pore size is nominally 1 nm[26]) to that in Accurel would be 200; whereas the experimental ratio is 27. Even at this ratio, it can be expected that the operating stability of OSN membranes is much better than microfiltration membranes.

Because the breakthrough pressure is low (1.1 bar, as shown in Table 2) for Accurel, the experiment was run carefully to avoid the aqueous solution or decanol leaking out through the membrane pores. The transmembrane pressure difference, based on the inlet pressures, was around 0.5 bar through the membrane sheet, with a higher pressure on the aqueous side for Accurel. For MPF 50, transmembrane pressure difference was controlled at 1.5 bar with the higher pressure on the aqueous side (3.5 bar in the inlet). As shown in Table 2, MPF 50 has a much higher breakthrough pressure than Accurel. Because silicone rubber is a nonporous membrane, there is no problem of pore breakthrough but a minimal pressure difference (around 0.5 bar) across the membrane was used to keep a flat shape. The typical pressure drop along each half-cell (inlet to outlet) was 1.5 bar on the aqueous side and 1.0 bar on the decanol side.

Time-Dependence Phenol Concentration Profiles and OMTCs

Figure 3 shows typical data for phenol concentrations on the aqueous and decanol sides with extraction through the membrane. With the assumption that the mass of phenol absorbed in the membrane is negligible, the mass balance

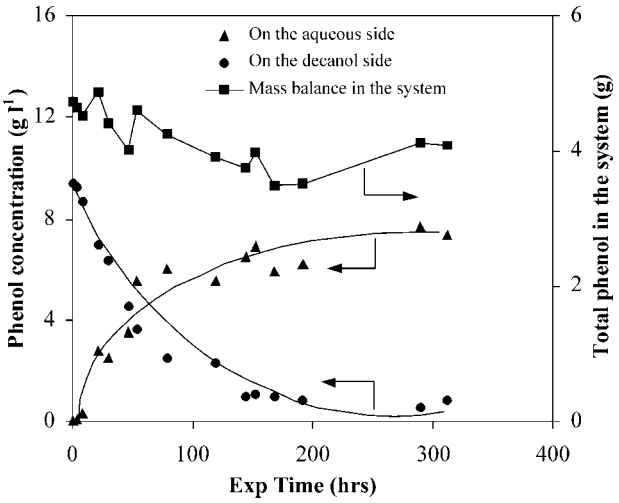

Figure 3. Variations of phenol concentration and phenol mass balance during transport through MPF 50.

of phenol in this system was checked by the following equation:

$$C^0_{aq}V_{aq} = C_{aq}V_{aq} + C_{org}V_{org} \tag{11}$$

The data of mass balance is also shown in Fig. 3. The system shows a good mass balance for phenol with an average deviation of $\pm 5\%$. Similar experimental data to that shown in Fig. 3 was obtained for all the other membranes involved in this study. Figure 4 summarizes this data by showing the change of normalized phenol concentrations with time on the aqueous side for all the membranes tested in this study.

The distribution coefficient of phenol between decanol and water was determined to be 20.6.[2] The experimental data in Fig. 4 can be used for the calculation of the OMTCs according to Eq. (9). A typical result is shown in Fig. 5, with a good linear relationship (correlation coefficient is 0.97). The OMTC is calculated from the slope. All the OMTCs obtained for phenol are shown in Table 3, along with the data obtained for partition coefficients of phenol between the various membranes and water.

It is clear from Table 3 that the OMTC of phenol in Accurel is much higher than the values for MPF 50 and silicone rubber. This is unsurprising, since Accurel possesses larger pores than the other membranes, and is the main reason why microfiltration membranes have widely been studied for MSE processes. Zha et al.[5] used a supported liquid membrane with decanol immobilized within the membrane with the same pore size as Accurel to extract phenol from aqueous solutions. The OMTC of phenol obtained by

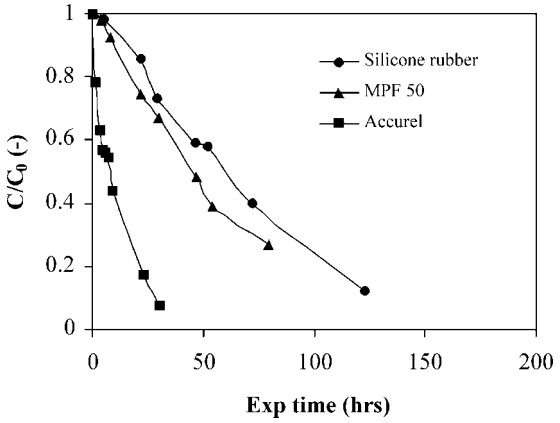

Figure 4. Variations of normalized concentrations of phenol on the aqueous side for different membranes. Effective membrane area in all tests was $0.015\,m^2$.

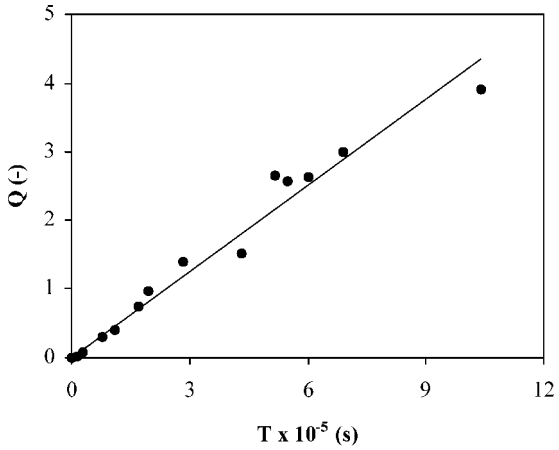

Figure 5. The calculation of OMTC of phenol in MPF 50, where $Q = \frac{1}{1+\beta}\ln\left(\frac{C_{aq,0}}{(1+\beta)C_{aq}-\beta C_{aq,0}}\right)$.

the researchers was around $3.4 \times 10^{-6}\,\mathrm{m\,s^{-1}}$, which is about 3 times higher than that in this study, mainly due to the fact that in their work, a thinner membrane of around 75 μm in thickness was employed and strong fluid turbulence was used to make liquid film resistances very low on both sides of the membrane.

Silicone rubber shows the worst performance in terms of the OMTC of phenol. As mentioned in the introductory section, nonporous membranes have a different separation mechanism from porous membranes, that is, the mass transfer rate in nonporous membranes mainly depends on the affinity between the membrane and penetrant. Because phenol is hydrophilic and silicone rubber is hydrophobic (the membrane-phenol partition coefficient is 0.3), a low OMTC of phenol is expected in silicone rubber.

Table 3. Overall mass transfer coefficients and partition coefficients of phenol and toluene in the membranes studied in the MSE.

	(Water-phenol)-decanol		(Water-toluene)-decanol	
Membrane	$k_{ov}^{aq} \times 10^7$, $\mathrm{m\,s^{-1}}$	P_{aq}^{mem}	$k_{ov}^{aq} \times 10^7$, $\mathrm{m\,s^{-1}}$	P_{aq}^{mem}
Accurel	12	0	38	16
MPF 50	1.3	1.3	23	37
Silicone rubber	0.6	0.3	77	234

MPF 50 has an OMTC of phenol that is intermediate between microfiltration and nonporous membranes. However, as shown in Table 2, MPF 50 possesses a much higher breakthrough pressure than Accurel. With the consideration of OMTC, breakthrough pressure, and solvent resistance, OSN membranes might be preferred if the operating stability of the system takes priority in some processes.

Comparison of OMTCs of Phenol and Toluene

Figure 6 shows the change of toluene concentrations in the aqueous and decanol solutions with time and the mass balance of toluene during extraction. This system shows a good mass balance for toluene with an average deviation of $\pm 10\%$. The change of normalized toluene concentrations with time on the aqueous side in Fig. 7 for all the membranes involved in this study is shown. OMTCs of toluene in these membranes were calculated in the same way for phenol, and the typical calculation of the OMTC of toluene is presented in Fig. 8. The values of OMTCs of toluene are also listed in Table 3, along with the data obtained for partition coefficients of toluene between the various membranes and water.

It can be seen in Table 3 that silicone rubber shows a higher OMTC of toluene than Accurel and MPF 50. This is mainly due to the fact that toluene

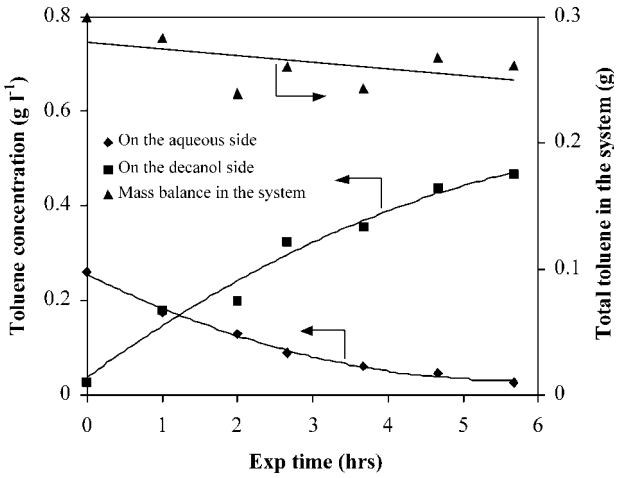

Figure 6. Variations of toluene concentration and toluene mass balance during transport through silicone rubber.

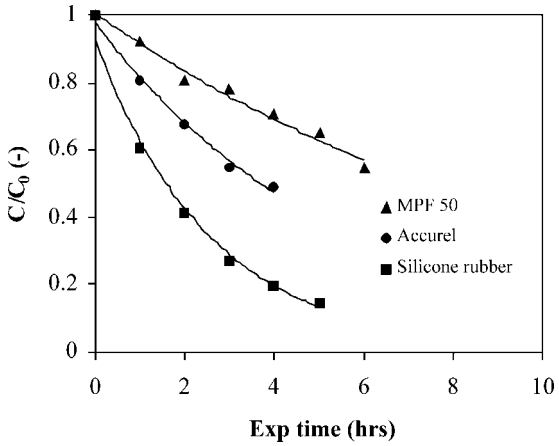

Figure 7. Variations of normalized concentration of toluene on the aqueous side for different membranes. Effective membrane area in all tests was 0.015 m^2.

has a strong affinity to silicone rubber with a partition coefficient of 234. As shown in Table 3, the partition coefficient of toluene between silicone rubber and water is much higher than that between Accurel and water.[16] Because MPF 50 contains a support layer, the partition coefficient of toluene between

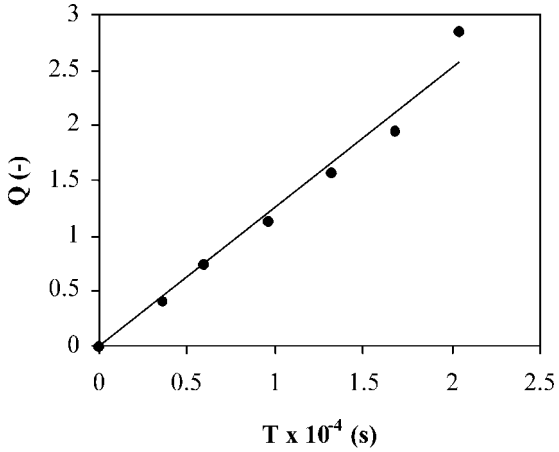

Figure 8. The calculation of OMTC of toluene in silicone rubber, and $Q = \frac{1}{1+\beta}\ln\left(\frac{C_{aq,0}}{(1+\beta)C_{aq}-\beta C_{aq,0}}\right)$.

the actual active layer and water could not be measured. The value shown is for qualitative use only as it reflects partitioning between the support and active layer and water. In silicone rubber, the OMTC of toluene is higher than the value of phenol by around two orders of magnitude. This is due to the difference in the partition coefficient for these two solutes.

For porous membranes, the medium in the pores is decanol. The diffusion coefficients of phenol and toluene in decanol were calculated according to the Wilke–Chang equation[27] and are shown in Table 1. To clarify the transport within Accurel, an analysis of the contributions of the transport through the membrane material and through the pores to the effective diffusion coefficient in the membrane D_e in Eq. (4) was made by using the values of the parameters given below:

$$\varepsilon \sim 0.6^{[2]}$$

$$\tau \sim 2^{[2]}$$

$$D_{mem} \sim 10^{-11}\,\mathrm{m^2\,s^{-1}}\ ^{[14]}$$

$$D_{pore} = 1.22 \times 10^{-10}\,\mathrm{m^2\,s^{-1}} \text{ for phenol and}$$

$$1.23 \times 10^{-10}\,\mathrm{m^2\,s^{-1}} \text{ for toluene}^{[27]}$$

$$P_{org}^{mem} = 0 \text{ for phenol and } 0.2 \text{ for toluene}$$

For the phenol system

$$(1 - \varepsilon) D_{mem} P_{org}^{mem} = 0$$

and

$$\frac{D_{pore}\varepsilon}{\tau} = 3.7 \times 10^{-11}\,\mathrm{m^2\,s^{-1}}$$

For toluene system

$$(1 - \varepsilon) D_{mem} P_{org}^{mem} \sim 0.1 \times 10^{-11}\,\mathrm{m^2\,s^{-1}}$$

and

$$\frac{D_{pore}\varepsilon}{\tau} = 3.7 \times 10^{-11}\,\mathrm{m^2\,s^{-1}}$$

The analysis shows that for Accurel, the contribution of transport through the membrane material to the effective diffusion coefficient in the membrane D_e is negligible for both phenol and toluene.

The conclusion is justified by analyzing experimental data in light of Eq. (3). Membrane resistances for both phenol and toluene systems were

calculated from experimental data, as shown in the Appendix. It was found that the experimental ratio of $(D_e P_{aq}^{org})_{\text{toluene}}$ and $(D_e P_{aq}^{org})_{\text{phenol}}$ is 3.5. According to Eq. (4), this ratio would be 3.9, with an assumption that the mass transport of phenol and toluene only takes place within the pores through Accurel. This result is consistent with the previous theoretical analysis.

The partition coefficients of phenol and toluene are not available between the active layer in MPF 50 and water, hence, quatitative analysis cannot be used here. However, we measured the partition coefficients of phenol and toluene between water and MPF 50, including the active layer and the support layer, and the data are shown in Table 3. It can be seen that the partition coefficient of toluene is higher than the value of phenol. This suggests that toluene has a good affinity for the membrane materials used in MPF 50.

Applying the same analysis as for Accurel, the experimental ratio of $(D_e P_{aq}^{org})_{\text{toluene}}$ and $(D_e P_{aq}^{org})_{\text{phenol}}$ is 20 for MPF 50. However, according to Eq. (4), this ratio would only be 3.9 under the assumption that the mass transport of phenol and toluene only takes place within liquid-filled pores in MPF 50. This is explained as follows. For Accurel, the ratio of $(D_e P_{aq}^{org})_{\text{toluene}}$ and $(D_e P_{aq}^{org})_{\text{phenol}}$ is almost exactly as we would expect based on the liquid–liquid partitioning between water and decanol. The solute–membrane interactions are not important. For MPF 50, the ratio of $(D_e P_{aq}^{org})_{\text{toluene}}$ and $(D_e P_{aq}^{org})_{\text{phenol}}$ is much higher than that we would expect from liquid–liquid partitioning. Toluene has a significantly higher affinity for the membrane materials than the phenol. It can be concluded that the interactions between the membrane material and the solute make a significant contribution to the mass transport of toluene in MPF 50.

Figure 9 shows the top-layer and support-layer structures of MPF 50 by scanning electron microscopy (SEM). Pores which, if they exist, are expected to be nominally 1 nm.[26] They are not visible under the SEM instrument used in this study; whereas, the support layers show clear pores and high porosity. In comparison, Fig. 10 shows the SEM photographs of Accurel, which display the clear porous top and support layers with a high porosity. Because the top layers of OSN membranes are very thin and have a density—either with or without real pores—between that of microfiltration membranes and nonporous membranes, it may be expected that mass transport through the top layer of MPF 50 combines characteristics through microfiltration and nonporous membranes.

According to the data for bond lengths and angles for gas-phase molecules in published experimental results,[28] the largest molecular dimension is roughly calculated to be 6.2 Å for phenol and 6.5 Å for toluene (kinetic diameter: 5.92 Å[29]). Unhindered diffusion through pores of the membrane exists only if the membrane pore size is at least two orders of

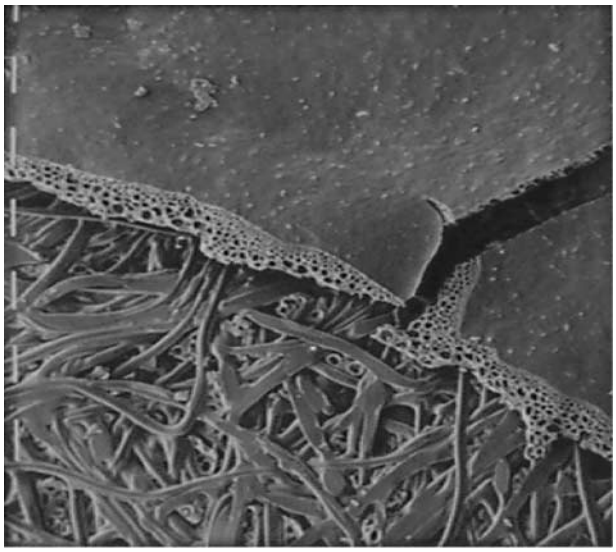

(a)

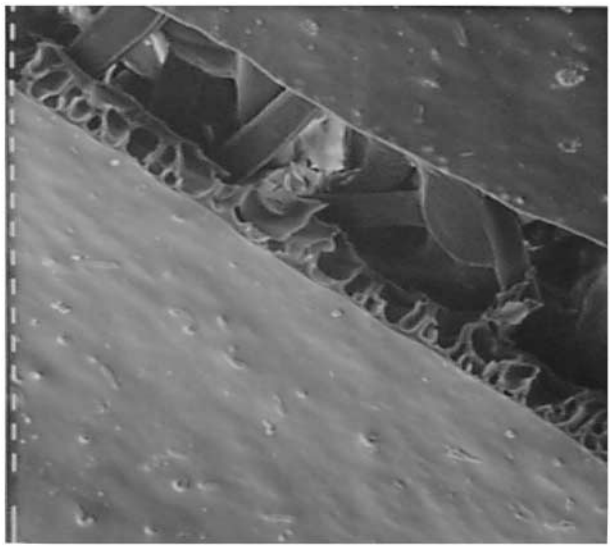

(b)

Figure 9. SEM photographs of MPF 50, (a) scale bar: 100 μm; (b) scale bar: 10 μm.

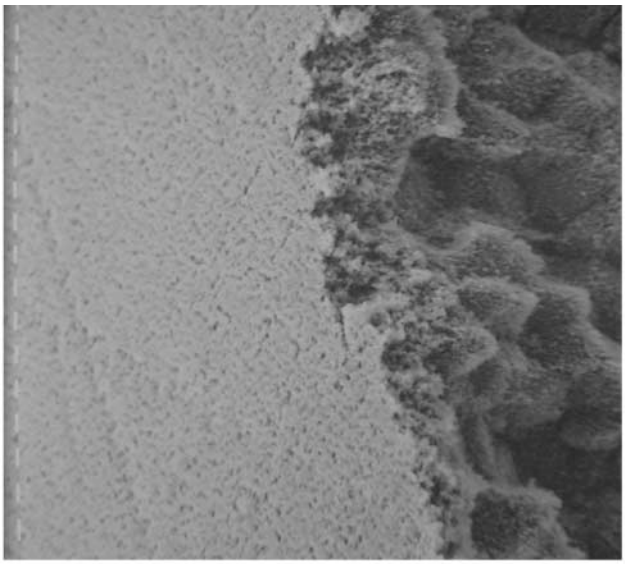

(a)

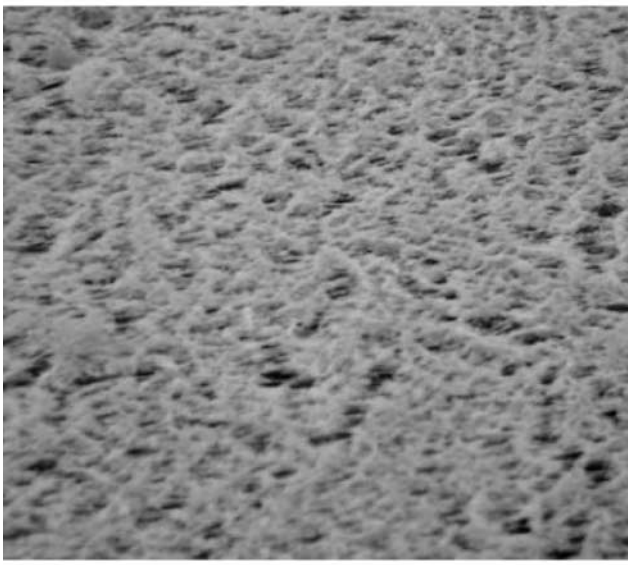

(b)

Figure 10. SEM photographs of Accurel, (a) scale bar: 10 μm; (b) magnification: 1250.

magnitude higher than the solute molecular dimensions.[5] Therefore, for MPF 50, the interactions of phenol and toluene with the walls of any pores would be dominant in the diffusion process. This means that the diffusion through the actual material of the top layer, or/and along the surfaces of pores, in the top layer, makes important contributions to mass transfer in OSN membranes. This result is interesting for considering the application of these kinds of membranes in separations where pure organic solvents, such as toluene, are forced through the membranes under pressure.

CONCLUSION

In MSE of phenol from water, OSN membrane MPF 50 has an intermediate OMTC between microfiltration membrane Accurel and nonporous membrane silicone rubber but a much higher breakthrough pressure than Accurel. Therefore, OSN membranes should be a good choice in the MSE, with a compromise between the OMTC and operating stability.

For porous membranes, the higher partition coefficient of the compound between organic solvent and water contributes to a higher OMTC. For hydrophobic OSN membrane MPF 50, diffusion through the membrane of the top layer or/and along the surfaces of pores in the top layer is a more important contributor to mass transport than diffusion of solutes in liquid-filled pores. This has implications for the mechanisms of separations via OSN membranes, in particular whether pure solvents pass through the membranes by pore flow or solution diffusion.

APPENDIX

The Lévèque correlation Eq. (A1) is often used to predict the liquid–film mass transfer coefficient for laminar pipe flow[11]

$$Sh = 1.62\, Re^{\frac{1}{3}} Sc^{\frac{1}{3}} \left(\frac{d_{eq}}{L}\right)^{\frac{1}{3}} \quad \mathrm{Re} < 2000 \tag{A1}$$

In this study, the equivalent diameter for the rectangular duct is

$$d_{eq} = \frac{4 \times Cross\text{-}sectional\ \ area}{Perimeter} = 9.23 \times 10^{-3}$$

For all experiments in this study, on the aqueous side of the membrane, the

superficial liquid velocity was

$$U_{aq} = 3.42 \times 10^{-2} \tag{A2}$$

and on the decanol side

$$U_{org} = 5.13 \times 10^{-3} \tag{A3}$$

From Eq. (A1), liquid–film resistances are 3.9×10^4 ($\frac{1}{k_{aq}}$) on the aqueous side and 9.3×10^4 ($\frac{1}{k_{org}P_{aq}^{org}}$) on the decanol side for experimental systems with phenol as the solute, and 4×10^4 ($\frac{1}{k_{aq}}$) and 2.4×10^4($\frac{1}{k_{org}P_{aq}^{org}}$) for experimental systems with toluene as the solute. The distribution coefficient of toluene between decanol and water was measured to be 81 in this study. In Accurel, the second term membrane resistance on the right side of Eq. (3) for the phenol system is

$$\frac{l}{D_e P_{aq}^{org}} = 7 \times 10^5 \tag{A4}$$

and

$$\frac{l}{D_e P_{aq}^{org}} = 2 \times 10^5 \tag{A5}$$

for the toluene system.

NOMENCLATURE

A	apparent area of the membrane sheet (m^2)
C_{aq}	bulk concentration on the feed side ($g\,l^{-1}$)
$C_{aq,0}$	initial concentration on the feed side ($g\,l^{-1}$)
C_{aq}^{*}	interfacial concentration on the feed side ($g\,l^{-1}$)
C_{mem}^{aq}	interfacial concentration in the membrane material of aqueous side ($g\,l^{-1}$)
C_{pore}^{aq}	interfacial concentration in the membrane pore of aqueous side ($g\,l^{-1}$)
C_{org}	bulk concentration on the organic side ($g\,l^{-1}$)
C_{org}^{*}	interfacial concentration on the organic side ($g\,l^{-1}$)
C_{mem}^{org}	interfacial concentration in the membrane material of organic side ($g\,l^{-1}$)
C_{pore}^{org}	interfacial concentration in the membrane pores of organic side ($g\,l^{-1}$)
d_{eq}	equivalent diameter (m)

D_e	effective diffusion coefficient in the membrane ($m^2\,s^{-1}$)
D_{mem}	diffusion coefficient through the membrane material ($m^2\,s^{-1}$)
D_{pore}	diffusion coefficient inside the membrane pores ($m^2\,s^{-1}$)
F	flow rate ($g\,s^{-1}$)
l	thickness of the membrane sheet (m)
k_{aq}	liquid–film mass transfer coefficient on the aqueous side ($m\,s^{-1}$)
k_{org}	liquid–film mass transfer coefficient on the organic side ($m\,s^{-1}$)
k_{ov}^{aq}	overall mass transfer coefficient based on the aqueous side($m\,s^{-1}$)
P	permeability ($m^2\,s^{-1}$)
P_b	breakthrough pressure (Pa)
P_{aq}^{mem}	partition coefficient between membrane and aqueous solution (−)
P_{aq}^{org}	distribution coefficient between organic solvent and aqueous solution (−)
P_{org}^{mem}	partition coefficient between membrane and organic solvent (−)
r	capillary radius (m)
Re	Reynolds number, $\frac{d_{eq}U\rho}{\mu}$(−)
Sc	Schmit number, $\frac{\mu}{\rho D}$(−)
Sh	Sherwood number, $\frac{kd_{eq}}{D}$(−)
t	time (s)
U_{aq}	superficial liquid velocity on the aqueous side ($m\,s^{-1}$)
U_{org}	superficial liquid velocity on organic side ($m\,s^{-1}$)
V_{aq}	volume of aqueous solution (m^{-3})
V_{org}	volume of organic solvent (m^{-3})

Greek Symbols

β	defined by Eq.(9) (−)
γ	interfacial tension ($N\,m^{-1}$)
ε	porosity of the membrane sheet (−)
τ	tortuosity of the membrane sheet (−)
μ	viscosity ($kg\,m^{-1}\,s^{-1}$)
ρ	density of liquid ($g\,m^{-3}$)
θ	contact angle (−)

ACKNOWLEDGMENTS

This work was funded by the United Kingdom Engineering and Physical Sciences Research Council (EPSRC), grant number GR/M50751.

REFERENCES

1. Mulder, M. *Basic Principles of Membrane Technology*, 2nd Ed.; Kluwer Academic Publishers: The Netherlands, 1996.
2. Prasad, R.; Sirkar, K.K. Solvent extraction with microporous hydrophilic and composite membranes. Am. Inst. Chem. Eng. J. **1987**, *33*, 1057–1066.
3. Prasad, R.; Sirkar, K.K. Dispersion free solvent extraction with microporous hollow fibre modules. Am. Inst. Chem. Eng. J. **1988**, *34* (2), 177–188.
4. Basu, R.; Prasad, R.; Sirkar, K.K. Nondispersive membrane solvent back extraction of phenol. Am. Inst. Chem. Eng. J. **1990**, *36* (3), 450–460.
5. Zha, F.F.; Fane, A.G.; Fell, C.J.D. Phenol removal by supported liquid membranes. Sep. Sci. Technol. **1994**, *29* (17), 2317–2343.
6. Baudot, A.; Floury, J.; Smorenburg, H.E. Liquid–liquid extraction of aroma compounds with hollow fibre contactor. Am. Inst. Chem. Eng. J. **2001**, *47* (8), 1780–1793.
7. Marx, S.; Weber, M.E. Extraction of a dissolved organic contaminant from water into an aqueous surfactant solution across a microporous membrane. Can. J. Chem. Eng. **2002**, *80* (2), 224–230.
8. Pierre, F.X.; Souchon, I.; Athes-Dutour, V.; Marin, M. Membrane-based solvent extraction of sulfur aroma compounds: influence of operating conditions on mass transfer coefficients in a hollow fibre contactor. Desalination **2002**, *148* (1–3), 199–204.
9. Kubisova, L.; Sabolova, E.; Schlosser, S.; Martak, J.; Kertesz, R. Membrane based solvent extraction and stripping of a heterocyclic carboxylic acid in hollow fibre contactors. Desalination **2002**, *148* (1–3), 205–211.
10. Lee, L.T.; Ho, W.S.; Liu, K.J. Membrane Solvent Extraction. US Patent 3,956,112, May 11, 1976.
11. Brookes, P.R.; Livingston, A.G. Aqueous-aqueous extraction of organic pollutants through tubular silicone rubber membranes. J. Membr. Sci. **1995**, *104*, 119–137.

12. Netke, S.A.; Pangarkar, V.G. Extraction of naphthenic acid kerosene using porous and nonporous polymeric membranes. Sep. Sci. Technol. **1996**, *31* (1), 63–76.
13. Ray, S.K.; Sawant, S.B.; Joshi, J.B.; Pangarkar, V.G. Perstraction of phenolic compounds from aqueous solution using a nonporous membrane. Sep. Sci. Technol. **1997**, *32* (16), 2669–2683.
14. Doig, S.D.; Boam, A.T.; Livingston, A.G.; Stuckey, D.C. Mass transfer of hydrophobic solutes in solvent swollen silicone rubber membranes. J. Membr. Sci. **1999**, *154*, 127–140.
15. Cocchini, U.; Nicolella, C.; Livingston, A.G. Countercurrent transport of organic and water molecules through thin film composite membranes in aqueous-aqueous extractive membrane processes. Part I: experimental characterisation. Chem. Eng. Sci. **2002**, *57* (19), 4078–4098.
16. Hauser, B.; Popp, P.; Kleine-Benne, E. Membrane-assisted solvent extraction of triazines and other semi-volatile contaminants directly coupled to large-volume injection-gas chromatography—mass spectrometric detection. J. Chromatogr. A **2002**, *963*, 27–36.
17. Machado, D.R.; Hasson, D.; Semiat, R. Effect of solvent properties on permeate flow through nanofiltration membranes. Part I. Investigation of parameters affecting solvent flux. J. Membr. Sci. **1999**, *163*, 93–102.
18. Machado, D.R.; Hasson, D.; Semiat, R. Effect of solvent properties on permeate flow through nanofiltration membranes. Part II. Transport model. J. Membr. Sci. **2000**, *166*, 63–69.
19. Whu, J.A.; Baltzis, B.C.; Sirkar, K.K. Nanofiltration studies of larger organic microsolutes in methanol solutions. J. Membr. Sci. **2000**, *170*, 159–172.
20. Yang, X.J.; Livingston, A.G.; Freitas dos Santos, L. Experimental observations on nanofiltration in organic solvents. J. Membr. Sci. **2001**, *190*, 45–55.
21. White, L.S. Transport properties of a polyimide solvent resistant nanofiltration membrane. J. Membr. Sci. **2002**, *205*, 191–202.
22. Bhanushali, D.; Kloos, S.; Bhattacharyya, D. Solute transport in solvent-resistant nanofiltration membranes for non-aqueous systems: experimental results and the role of solute-solvent coupling. J. Membr. Sci. **2002**, *208*, 343–359.
23. Van der Bruggen, B.; Greens, J.; Vandecasteele, C. Influence of organic solvents on the performance of polymeric nanofiltration membranes. Sep. Sci. Technol. **2002**, *37* (4), 783–797.
24. Han, S.J.; Ferreira, F.C.; Livingston, A.G. Membrane aromatic recovery system (MARS)—a new membrane process for the recovery of phenols from wastewaters. J. Membr. Sci. **2001**, *188*, 219–233.

25. Zha, F.F.; Fane, A.G.; Fell, C.J.D.; Schofield, R.W. Critical displacement pressure of a supported liquid membrane. J. Membr. Sci. **1992**, *75*, 69–80.
26. Bowen, W.R.; Welfoot, J.S. Modelling the performance of membrane nanofiltration—critical assessment and model development. Chem. Eng. Sci. **2002**, *57* (7), 1121–1137.
27. Wilke, C.R.; Chang, P. Correlation of diffusion coefficients in dilute solutions. Am. Inst. Chem. Eng. J. **1955**, *1* (2), 264–270.
28. Lide, D.R. *Handbook of Chemistry and Physics*; 76th Ed. CRC Press: USA, 1995, 1996.
29. Hippler, H.; Troe, J.; Wendelken, H.J. Collisional deactivation of vibrationally highly excited polyatomic molecules II. Direct observations for excited toluene. J. Chem. Phys. **1983**, *78* (1), 6709–6717.

Received October 2002
Revised January 2003